

COMPRESSION OF FREQUENCY-MODULATED ELECTROMAGNETIC PULSES IN SECTIONS OF REGULAR WAVEGUIDES

V.L. Pazyinin

*A. Usikov Institute of Radio Physics and Electronics,
National Academy of Sciences of Ukraine
12, Academician Proskura St., Kharkiv 61085, Ukraine
E-mail: pazyinin@ire.kharkov.ua*

The paper suggests an efficient algorithm for rigorous calculation of the transformation of the waveform of electromagnetic pulses propagating in regular waveguides. The algorithm is applied to analyzing the possibility of passive compression of frequency-modulated pulses.

KEY WORDS: *frequency-modulated pulses, pulse compression, regular waveguide sections, convolution integral*

1. INTRODUCTION

The idea of passive compression of radio-frequency pulses has been formulated rather long ago (see, for example, papers [1–6]). Let a pulse modulated according to a certain law in frequency and amplitude be fed at the input of a dispersive waveguiding section. Then it is quite possible that all frequency components of the pulse would arrive at a certain spatial point simultaneously (in a certain sense of this word) and in-phase. The effect would be accompanied by an increase in the pulse amplitude, while decrease in its length (for example, at a given power level). The main theoretical problem which should be solved in this situation consists in determining the law of amplitude and frequency modulation of the primary pulse required for the given dispersive system. Despite the apparent simplicity of this problem and a great number of performed theoretical and experimental studies (see, for example, [1-13]), the results obtained by today seem to be rather modest. For example, the attained compression factor, i.e., the input-to-output pulse length ratio, equals to several dozens at the best. The progress observed in this field over the recent fifty years concerns transition to shorter operation wavelengths rather than increase in the compression factor. In the author's opinion this situation is most likely explained by the insufficient quality of the used mathematical models which should precede real physical

experiments. The main and common shortcoming characteristic for perhaps all the works the author has known is the explicit or implicit use of the so-called kinematical approximation (see, for example, [10]), within which the input pulse is represented (often purely conceptually) as a continuous chain of “particle” (wave packets) entering the dispersive element of the compressor each with its own time delay. On assumption (again without any foundation) that the frequency dependence of the “particle” speed coincides with the dispersion law pertaining to the compressor the pure kinematic equations of motions are used to determine both the time delays, i.e., the law of frequency modulation of the input pulse, and the “optimum” length of the dispersive element, i.e., such a distance after passage of which all the “particles” meet at one point. Undoubtedly, such a kinematic representation is useful for qualitative description of the physical processes occurring in a compressor. However, as it will be shown below, it proves to be a very rough approximation and is inapplicable for rigorous modeling and synthesis of specific radiophysical devices.

In the present paper the possibility of electromagnetic pulse compression in regular homogeneous waveguides of arbitrary transverse cross-section is analyzed theoretically. The main advantage of the approach developed here is the use of rigorous methods for calculation of electrodynamic characteristics of the operating pulse and accurate performance of numerical experiments the results of which can be repeated in real physical devices if it is necessary. The main idea for determining the required modulation laws consists in solving preliminarily the “inverse” problem as follows. If we know the pulse form to be obtained in the result, then applying it to the output of the dispersive system and changing the time variable t by $-t$ we will obtain the input pulse of the system within an accuracy to the reverse change of $-t$ with t . Once the time profile of the input signal has been found, there is no problem to determine the laws of its modulation. Such a way of carrying out numerical experiments was first suggested in paper [14]. It is a universal scheme applicable to any (at least linear ones) dispersive media or waveguiding systems.

2. TRANSPORT OPERATORS FOR REGULAR WAVEGUIDES

The well-known [15] dependence of the group velocity v on frequency k

$$v(k) = v\sqrt{1 - (k_n/k)^2} \quad (1)$$

suggests that the effect of compression of frequency-modulated pulses can be observed even in such a simplest dispersive system like a regular waveguide. Here v is the wave propagation velocity in the medium filling the waveguide and k_n is the waveguide cutoff frequency. For numerical modeling of this effect it is necessary to have robust and efficient algorithms capable of calculating transformations of the time profile of a pulse in the course of its motion through the waveguide. Papers [16-22]

suggest the transport operators relating electromagnetic fields in two arbitrary cross-sections of a hollow regular semi-infinite waveguide with perfectly conducting walls. If the waveguide is filled by a medium characterized by the specific permittivity ε , permeability μ and conductivity σ , then these operators for the space-and-time amplitudes $u_n(z, t)$ of any transverse component of the field take the form

$$u_n(z, t) = \mp \frac{1}{\sqrt{\varepsilon\mu}} \int_0^{t-\sqrt{\varepsilon\mu}|z-z_0|} \frac{\partial u_n(z_0, \tau)}{\partial z} \cdot \exp(-s(t-\tau)) J_0\left(\eta_n \sqrt{(t-\tau)^2 - \varepsilon\mu(z-z_0)^2}\right) d\tau, \quad (2)$$

$$u_n(z, t) = \mp \frac{1}{\sqrt{\varepsilon\mu_0}} \int_0^t \frac{\partial u_n(z, \tau)}{\partial z} \cdot \exp(-s(t-\tau)) J_0(\eta_n(t-\tau)) d\tau, \quad (3)$$

$$\frac{\partial u_n(z, t)}{\partial z} = \mp \sqrt{\varepsilon\mu} \left[\frac{\partial u_n(z, t)}{\partial t} + s u_n(z, t) \right] + \eta_n \int_0^t \frac{\partial u_n(z, \tau)}{\partial z} \cdot \exp(-s(t-\tau)) J_1(\eta_n(t-\tau)) d\tau, \quad (4)$$

$$\frac{\partial u_n(z, t)}{\partial z} = \mp \sqrt{\varepsilon\mu} \left[\frac{\partial u_n(z, t)}{\partial t} + s u_n(z, t) + \eta_n \int_0^t u_n(z, \tau) \exp(-s(t-\tau)) \frac{J_1(\eta_n(t-\tau))}{t-\tau} d\tau \right]. \quad (5)$$

Here z is supposed to be the longitudinal axis of the waveguide and the upper and lower signs correspond to waves propagating toward increasing and decreasing z , respectively. In addition $s = \sigma\eta_0/2\varepsilon$, $\eta_n = \sqrt{\lambda_n^2/\varepsilon\mu - s^2}$ ($\lambda_n \geq \varepsilon\mu s^2$) and $\eta_0 = \sqrt{\mu_0/\varepsilon_0}$, with ε_0 and μ_0 being the free space permittivity and permeability, respectively. The “time” t has dimension of length since it is a product of the real time by the velocity of light in free space. Dimensions of other values correspond to the SI system. Magnitudes of the transverse eigenvalues λ_n are dependent on the waveguide type and wave polarization and can be calculated analytically for waveguides with the simplest cross-section geometry. For example [22], for a parallel-plate waveguide of height a we have $\lambda_n = n\pi/a$, $n = 1, 2, 3, \dots$ (TE_n -modes) and $\lambda_n = n\pi/a$, $n = 0, 1, 2, \dots$ (TM_n -modes). For a circular waveguide of radius b these are $\lambda_n = j_{1,n}/b$, $n = 1, 2, 3, \dots$ (TE_{0n} -modes) and $\lambda_n = j_{0,n}/b$, $n = 1, 2, 3, \dots$ (TM_{0n} -modes), where $j_{m,n}$ are roots of the Bessel function J_m ($J_m(j_{m,n}) = 0$). The eigenvalues λ_n for waveguides of more complex transverse cross-sections can be found using numerical methods.

The operators Eqs. (2) to (5) are exact in the sense that they strictly follow from the Maxwell equations. For this reason they can be used without any limitations for investigating evolution of a pulse with arbitrary waveform in the course of its motion through the waveguide. In particular, the spectrum of the signal under investigation can differ from zero at frequencies located both above and below the cutoff frequency.

In this case the operators Eqs. (2) through (5) are applicable as well and describe correctly transformations of the operating pulse waveform. To be convinced of that, let us rewrite Eq. (3) with infinite limits of integration, viz.

$$u_n(z, t) = \mp \int_{-\infty}^{\infty} \frac{\partial u_n(z, \tau)}{\partial z} \cdot K(\lambda_n(t - \tau)) d\tau, \quad K(t) = \begin{cases} J_0(t), & \text{if } t \geq 0 \\ 0, & \text{if } t < 0 \end{cases}. \quad (6)$$

For simplicity it has been assumed that $\varepsilon = \mu = 1$ and $\sigma = 0$, since the general case can be considered by analogy. Making use of the convolution theorem we obtain

$$\tilde{u}_n(z, k) = \mp \frac{\partial \tilde{u}_n(z, k)}{\partial z} \cdot \tilde{K}(k). \quad (7)$$

Here and throughout below in the paper the spectrum $\tilde{f}(k)$ of the signal $f(t)$ is calculated using the integral Fourier transform, viz.

$$\tilde{f}(k) = \frac{1}{2\pi} \int_{-\infty}^{\infty} f(t) e^{ikt} dt \quad \leftrightarrow \quad f(t) = \int_{-\infty}^{\infty} f(k) e^{-ikt} dk, \quad (8)$$

where $k = 2\pi/\lambda$, with λ being the free-space wavelength. Making use of the value of the integral [23]

$$\tilde{K}(k) = \int_0^{\infty} J_0(\lambda_n t) e^{ikt} dt = \begin{cases} (\lambda_n^2 - k^2)^{-1/2}, & \text{if } 0 < k < \lambda_n \\ i(k^2 - \lambda_n^2)^{-1/2}, & \text{if } 0 < \lambda_n < k \end{cases} \quad (9)$$

equation (7) can be brought to the familiar representation for electromagnetic wave frequency components in the waveguide

$$\tilde{u}_n(z, k) = \begin{cases} A(k) e^{\mp \beta z}, & \beta = \sqrt{\lambda_n^2 - k^2}, \quad \text{if } 0 < k < \lambda_n \\ A(k) e^{\pm i\beta z}, & \beta = \sqrt{k^2 - \lambda_n^2}, \quad \text{if } 0 < \lambda_n < k. \end{cases} \quad (10)$$

Here A is the constant of integration of the equation Eq. (7). Similar derivations can be carried out for the convolutions Eqs. (2), (4) and (5).

Thus, the operators Eqs. (2) to (5) describe correctly both the propagating and evanescent waves. This property is of prime importance for performance of numerical experiments. Any inaccuracy in specifying the time dependence of the input signal resulting in appearance of spectral components below the cutoff frequency proves to be not disastrous for the algorithm realizing the formulas Eqs. (2) to (5). All such

components will rapidly damp in the course of the pulse propagation through the waveguide as it occurs in reality.

Now let us formulate the main steps of the algorithm of recalculation of the time-dependent profile of the pulse $u_n(z_0, t)$ from one (reference) cross-section z_0 onto another arbitrary waveguide cross-section z . Let the initial signal $u_n(z_0, t)$ be specified within the time interval $0 \leq t \leq t_u$, whereas the output signal is to be determined for the time interval $0 \leq t \leq t_v$, $t_v \geq t_u$ (see Appendix). Since the initial function $u_n(z_0, t)$ is specified on a uniform time mesh with step h_t which is independent of the parameter η_n , it might occur, generally speaking, that the period T_J of Bessel function oscillations in the convolution would be comparable with or even smaller than the step h_t . For such values of the parameters η_n and h_t it becomes impossible to exactly calculate the integrals in Eqs. (2) to (5). For this reason to prevent the appearance of such situations let us introduce a parameter α to control the accuracy of mesh approximation of the Bessel function. If the condition

$$T_J/h_t \geq \alpha \quad (11)$$

holds, then the convolutions are calculated using the function $u_n(z_0, t)$ with the preset step h_t . Otherwise Eq. (11) is not met the function $u_n(z_0, t)$ is redefined for a finer mesh with such a step h_t that the inequality Eq. (11) would be met. In the latter case the missed values $u_n(z_0, t)$ can be obtained using interpolation formulas. It has been found experimentally that to provide the acceptable calculation accuracy it is sufficient to select α between 10^3 and 10^4 . The value T_J can be estimated using the asymptotic formula [23]

$$J_n(\eta_n t) \sim \sqrt{\frac{2}{\pi \eta_n t}} \cos\left(\eta_n t - \frac{n\pi}{2} - \frac{\pi}{4}\right); \quad T_J = 2\pi/\eta_n. \quad (12)$$

The algorithm for recalculation of the pulse waveform $u_n(z_0, t) \rightarrow u_n(z, t)$ includes the following basic steps.

1. Test of the prescribed function $u_n(z_0, t)$ for satisfying the condition Eq. (11) as has been described above.
2. Calculation of $\partial u_n(z_0, t)/\partial t$ for the time interval $0 \leq t \leq t_u$. To that end the formulas of numerical five-point first-order differentiation [24] were used in the present paper.
3. Calculation of $\partial u_n(z_0, t)/\partial z$ after the formula Eq. (5) for the time interval $0 \leq t \leq t_v$. It is assumed that $u_n(z_0, t) \equiv \partial u_n(z_0, t)/\partial t \equiv 0$ for $t_u < t \leq t_v$.

4. Calculation of $u_n(z, t)$ using the formula Eq. (2) for the time interval $0 \leq t \leq t_v$.

Calculation of the convolution integrals is the main difficulty which can arise in practical implementation of the described algorithm. The “direct” use of the quadrature trapezoid formulas, the Simpson rule etc. would require to perform about $O(M^2)$ (M is the size of the arrays to be convolved) floating-point operations which makes the formulas Eqs. (2) to (5) impractical in the case of rather long pulses. To solve this problem an algorithm has been suggested in paper [25] for calculating such convolutions using the Fast Fourier Transform (FFT) which requires about $O(M \log M)$ operations to be performed. In the present paper a modification of this algorithm was used whose description is presented in the Appendix.

3. PULSE COMPRESSION IN REGULAR WAVEGUIDES

Now consider the possibility of compression of frequency-modulated pulses in a regular waveguide using the algorithm described in the previous Section. The general scheme of the numerical experiment includes the following steps.

1. Selection of the pulse time-dependent profile which would be desirable to obtain at the compressor output.
2. Solution of the “inverse” problem. Knowing the pulse selected according to item 1 in the cross-section $z_0 = 0$ of the waveguide a segment of which we would like to use for constructing the power compressor, it is necessary to find its time profile at a given distance z from the reference cross-section z_0 .
3. Determination of the laws of amplitude and frequency modulation of the signal obtained in item 2.
4. Construction of the pulse using the modulation laws determined in item 3 and changing in it the time variable t by $-t$.
5. Solution of the “direct” problem. It is necessary to excite the pulse obtained in item 4 within the waveguide cross-section z_0 and calculate its time dependence at the distance z .

Selection of the pulse waveform to be finally obtained is determined by those problems for which solution each specific device is constructed. There is a great many of options here, however we will confine the present study, without the loss in generality of the analysis, to the following pulse

$$u_n(t) = A \cdot S(t) \cdot \cos(k_c(t-T)) \cdot \sin(k_s(t-T)) / (t-T), \quad t_{\min} \leq t \leq t_{\max}, \quad (13)$$

$$S(t) = x^2(3-2x); \quad \begin{cases} x(t) = (t-t_{\min}) / (t_1-t_{\min}); & t_{\min} \leq t \leq t_1 \\ 1; & t_1 < t < t_2 \\ x(t) = (t-t_{\max}) / (t_2-t_{\max}); & t_2 \leq t \leq t_{\max} \end{cases},$$

propagating in a regular homogeneous waveguide in the general case of arbitrary cross-section. Here $u_n(t)$ is the amplitude of one of the transverse components of the field and n is the number of the respective wave (see the formulas Eqs. (2) to (5)). The factor $S(t)$ composed of two splines has been introduced for convenience of calculations. It is intended for “smoothing” the source “edges” and makes it possible to more accurately calculate the time derivatives at the moments of source “switching on”, t_{\min} , and “switching off”, t_{\max} . The selection of such pulse waveform is easily explainable. With t_{\min} and t_{\max} going, respectively, to plus and minus infinity the amplitude spectrum of the signal $u_n(t)$ within the range $k_c \pm k_s$ tends to a constant level while vanishes outside of this range. For this reason the dependence Eq. (13) can be regarded as an approximate representation of the Dirac delta function whose spectrum is uniform within the range $-\infty < k < \infty$. The unique properties of the delta-function make it a key tool in the theoretical electrodynamics and signal processing theory, in particular, when investigating pulse responses of dynamic systems. For this reason it seems quite attractive to use at least its approximate analog in real physical devices as well. Let us select the following values of the parameters

$$A = 4, k_c = 6.25, k_s = 2.75, t_{\min} = t_0 = 0, t_1 = t_2 = T = 25, t_{\max} = t_3 = 50. \quad (14)$$

The time step of discrete representation of the function $u_n(t)$ is $h_t = 0.002$. The time-temporal dependence of the function Eq. (13) and its amplitude spectrum calculated for such parameters are shown in Figs. 1(a) and 1(b).

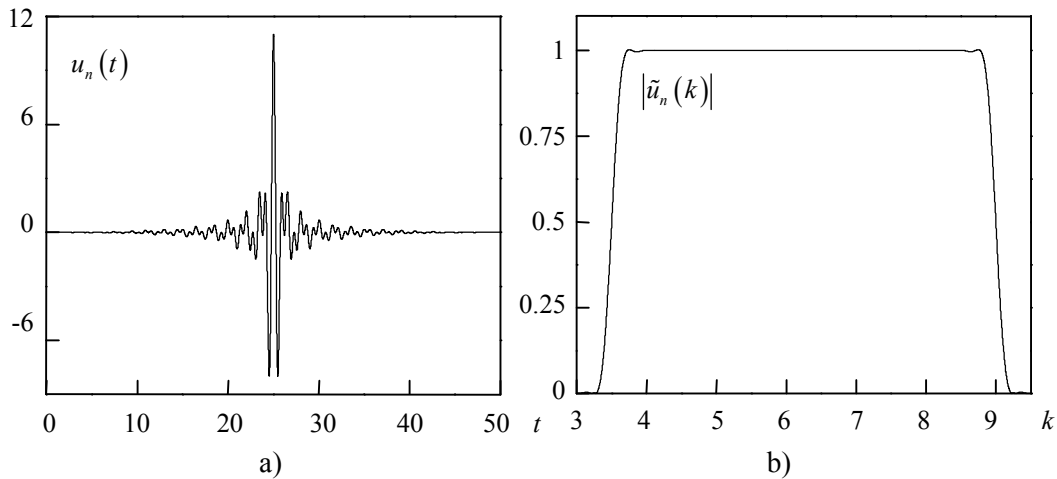


FIG. 1: Pulse determined by Eq. (13) with the selected parameters (a) and its amplitude spectrum (b)

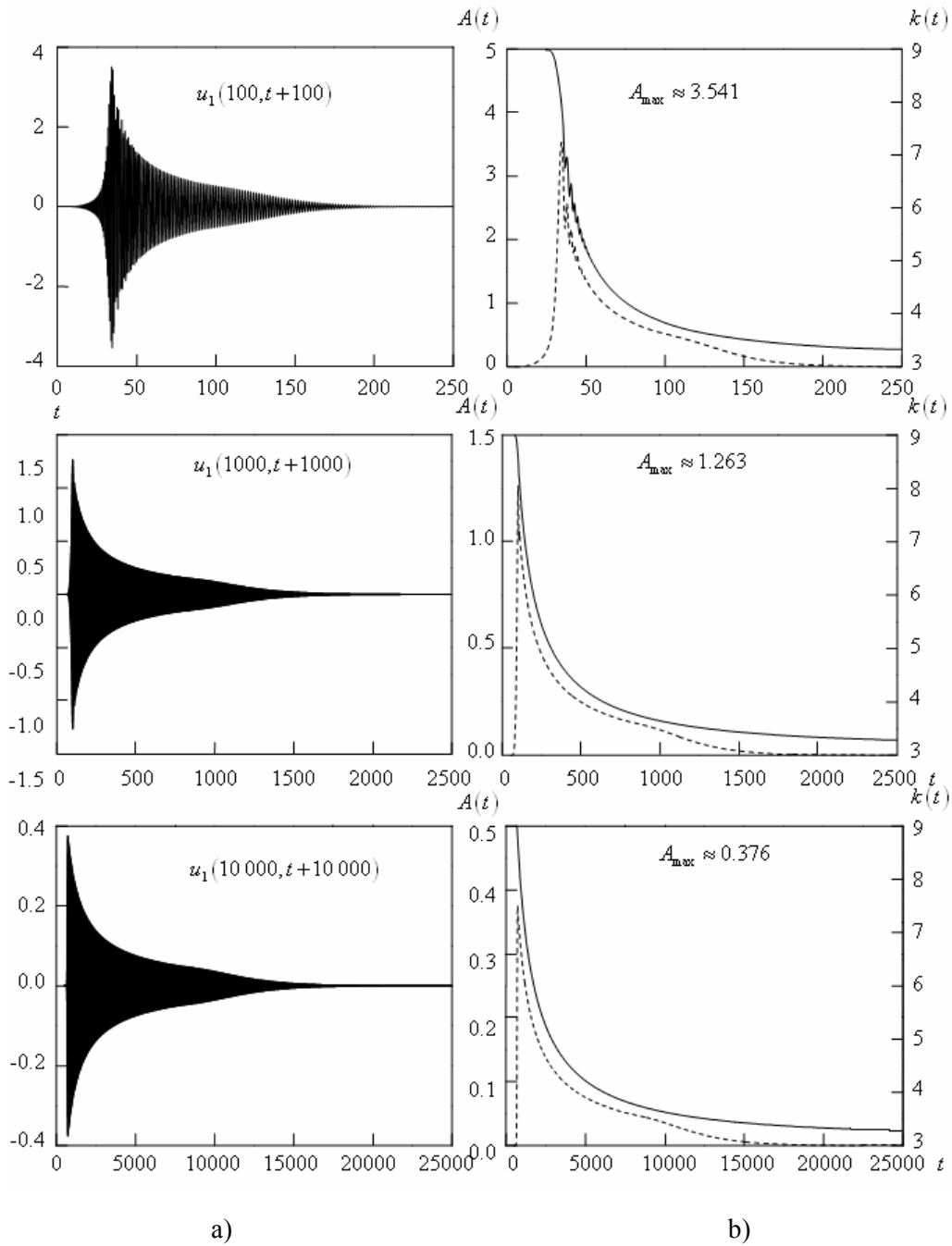


FIG. 2: The pulse at the distance 100, 1000 and 10000 m (waveguide heights) from the reference cross-section (a) and functions of its amplitude (dashed line) and frequency (solid line) modulation (b)

To solve the “inverse” problem it is necessary to specify the waveguide type and the operating mode. Since the dependence on the waveguide type in the formulas Eqs. (2) to (5) appears through the parameter η_n alone, it does not matter in principle what exactly waveguide has been selected in the capacity of the dispersive system. The final result will be the same for different waveguides with identical η_n . For this reason let us take, for specificity, a hollow ($\varepsilon = \mu = 1, \sigma = 0$) parallel-plate waveguide of height $a=1$ and investigate the transformation of the TE_1 -mode ($n=1$) in it. When the occasion requires the obtained results can be easily scaled to other types of waveguides with different transverse sizes. The cutoff frequencies of the selected waveguide equal $k_n = n\pi$, and the pulse spectrum (Fig. 1(b)) covers the range corresponding to single-mode and two-mode propagation in the waveguide. Figure 2(a) shows transformations of the pulse presented in Fig. 1(a), which has been initially excited within the reference cross-section $z_0 = 0$, corresponding to the cross-sections $z = 100, 1000$ и 10000 . For the selected scale along the t -axis oscillations of the function $u_1(z, t+z)$ are so dense that the area occupied by the pulse seems to be completely filled. More detailed information about these dependences can be obtained from the modulation laws (see below). As can be seen, the pulse length increases almost proportionally to the distance passed by the pulse. Therefore, increasing infinitely the waveguide segment length it is possible theoretically to construct a compressor with however large factor of compression of the input pulse. From the practical standpoint, all characteristics of the compressor will be confined due to loss associated with conduction currents in the waveguide walls.

Let us find the laws of amplitude $A(t)$ and frequency $k(t)$ modulation of the obtained pulses. The window Fourier transform

$$\tilde{f}(t, k) = \frac{1}{2\pi} \int_{t_{\min}}^{t_{\max}} f(\tau) W\left(\tau - t + \frac{w}{2}\right) e^{ik\tau} d\tau \tag{15}$$

makes it possible to visually represent signal changes in the coordinates of time-frequency and to check the carrier frequency for uniqueness. Figures 3(a) and 3(b) show results of applying the transformation Eq. (15), respectively, to the initial function $u_1(0, t)$ and the function $u_1(1000, t+1000)$ with the use of the Hamming window [26] $W(t) = 0.54 - 0.46 \cos(2\pi t/w)$ of width $w = 8$. Each spectrum in Fig. 3(b) has been calculated for the respective position of the time window and normalized to unity

$$\tilde{u}^{norm}(t, k) = \tilde{u}(t, k) / \max_k \tilde{u}(t, k). \tag{16}$$

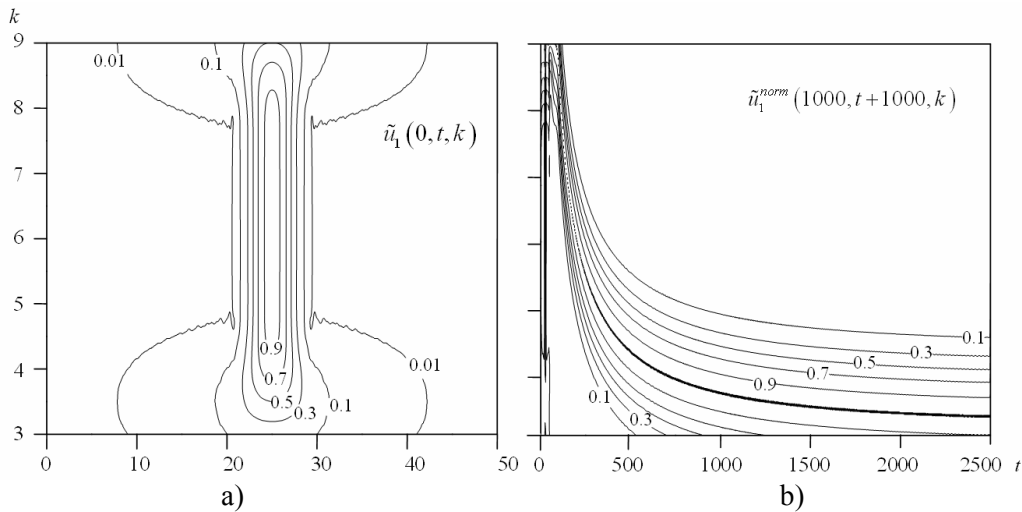


FIG. 3: Window Fourier transforms of the functions $u_1(0, t)$ (a) and $u_1(1000, t+1000)$ (b)

The thick curve corresponds to $\tilde{u}_1^{norm} = 1$ and actually demonstrates the frequency modulation law. However, it is not practical to apply the window transform Eq. (15) for determining the exact dependence $k(t)$ since it requires selecting too fine frequency step, using two-coordinate interpolation formulas etc. As a result, the complexity of the computer programs and computation time increase unjustifiably. In the present paper a simpler and more efficient technique was used instead to simultaneously find both the frequency and amplitude modulation laws. First, sequences of zeros s_1, s_2, \dots, s_N and extremes e_1, e_2, \dots, e_{N-1} of the wanted function $f(t)$ were determined within the given time interval $[\tilde{t}_0, \tilde{t}_1]$. The zeros and extremes were arranged according to the inequalities $\tilde{t}_0 \leq s_1 < e_1 < s_2 < \dots < s_i < e_i < s_{i+1} < \dots < e_{N-1} < s_N \leq \tilde{t}_1$. Then for every time moment e_i the amplitude and frequency were estimated by the following rule

$$A(e_i) = |f(e_i)| \text{ and } k(e_i) = \pi / (s_{i+1} - s_i). \quad (17)$$

The quadratic interpolation formulas were used if for further calibration it should be necessary to know the value of the amplitude and frequency for time moments which do not agree with e_i . The experience of numerical experimenting shows that this way of estimating the dependences $A(t)$ and $k(t)$ proves to be more efficient than using the window Fourier transform (more accurate results and shorter computation time).

Finally, to unambiguously recover the initial function $f(t)$ from the found modulation laws [27]

$$f'(t) = A(t) \sin \left(\varphi_0 + \int_{s_1}^t k(\tau) d\tau \right), \text{ with } s_1 \leq t \leq s_N \tag{18}$$

it also necessary to know the phase φ_0 of signal at the initial time moment. Since the reconstruction was performed for the interval $[s_1, s_N]$, we have $f'(s_1) = 0$, and $\varphi_0 = 0$ if $f(e_1) > 0$ and $\varphi_0 = \pi$ if $f(e_1) < 0$.

The described algorithm of determining the modulation laws and recovering from these the initial signal has been applied to the pulses $u_1(z, t+z)$ with $z = 100, 1000$ and 10000 (see Fig. 2(a)) and has provided acceptable results as for their accuracy. Figure 2(b) shows time dependences of the amplitudes (left scale) and frequencies (right scale) calculated for these pulses. Figure 4 presents time dependence of the absolute error $u_1(1000, t+1000) - u_1'(1000, t+1000)$ of recovering the signal $u_1(1000, t+1000)$. As can be seen the error is less by about three orders of magnitude than the value of the function itself (the integration in Eq. (18) was performed using the quadrature trapezoid formula).

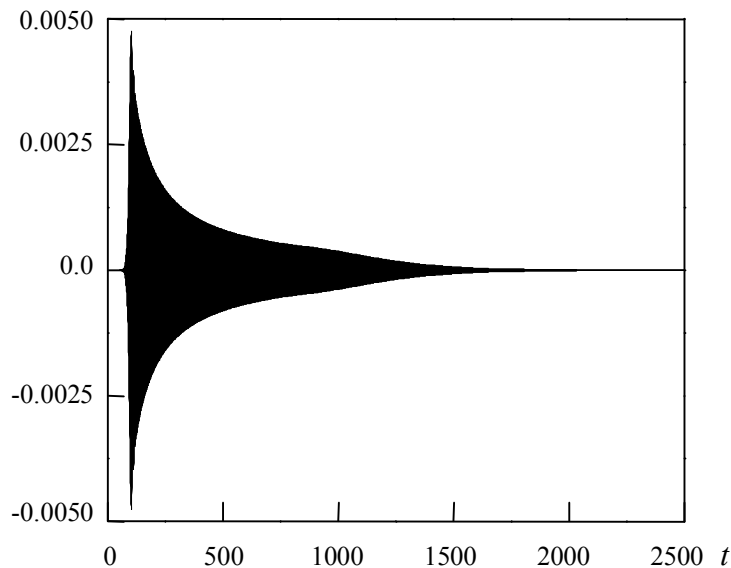


FIG. 4: Error of recovering the function $u_1(1000, t+1000)$ from the found laws of amplitude and frequency modulation

The presence appreciable oscillations in the signal amplitude and frequency at the distance $z = 100$ from the reference cross-section (Fig. 2(b)) indicates that the time “separation” of frequencies in the initial pulse has not yet occurred which makes it inconvenient for practical use. At greater z the frequency modulation law shows a monotonous character. Pulses of the kind are of greatest interest for the study.

The final step consists in recovering the desired pulse. To that end the signal $u_1'(z, t+z)$ ($s_1 \leq t \leq s_N$) is used to reconstruct the reversed in time signal $u_1''(t) = u_1'(z, s_N - t + z)$ ($0 \leq t \leq s_N - s_1$) which is to be excited within the reference cross-section of the waveguide $z_0 = 0$. The time profile of the reconstructed pulse within the cross-section z is described by a function which will be referred to as $u_1^*(z, t+z)$. The signals u_1'' and u_1^* for $z = 1000$ ($s_1 \approx 50.19$; $s_N \approx 2499.03$) are presented in Figs. 5(a) and 5(b), respectively. As can be seen from Fig. 1(a) the initial pulse u_1 has been reconstructed with a sufficiently high accuracy. The minor difference between u_1^* and u_1 is due to that we have truncated the long-lasting “ringing” tail of $u_1(1000, t+1000)$ for $t > 2500$. Increasing the length of $u_1(z, t+z)$ it is possible, at least in theory, to however accurately reproduce the profile of the desired signal.

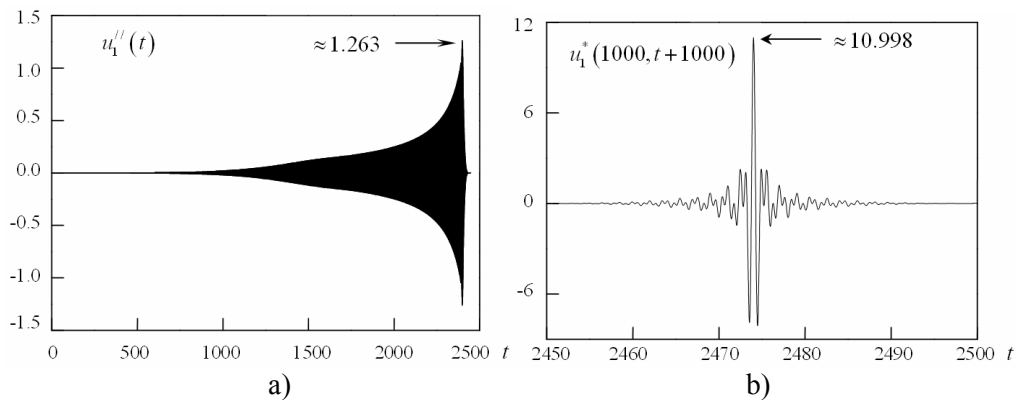


FIG. 5: The pulse within the reference cross-section of the waveguide $z_0 = 0$ (a) and its profile within the cross-section $z = 1000$ (b)

The compressor built around such waveguide section for to transform the pulse u_1'' into u_1^* will have the following characteristics.

- Amplitude gain (output-to-input signal maximum magnitude ratio)
 $\alpha = u_{\max}^* / u_{\max}'' \approx 10.998 / 1.263 \approx 8.708$.
- Compression factor (input-to-output pulse length ratio)
 $\beta = T'' / T^* \approx 2448.84 / 50 \approx 48.98$.

- Efficiency (output-to-input pulse power ratio) $\gamma = \int [u^*(t)]^2 dt / \int [u''(t)]^2 dt \approx 67.76947/67.76961 \approx 1$. Here the integrals are taken over time intervals corresponding to the lengths T^* and T'' of the respective pulses.
- Power gain (product of the compression factor by the efficiency) $\theta = \beta \cdot \gamma \approx 48.98$.

The above characteristics have been calculated with neglect of the loss due to the conduction currents in the waveguide walls.

Now it seems interesting to compare the modulation law obtained for the pulse $u_1(z, t+z)$ with that which could be expected proceeding from intuitive conception on propagation of the wave packets, by superposition of which the initial signal Eqs. (13) and (14) can be represented, through a dispersive system. If each of these packets is sufficiently narrowband near the frequency k and they all at the time moment t_0 ($t_0 \geq 0$) are located within the reference cross-section $z_0 = 0$ (as follows from Fig. 3(a) it is a plausible assumption), then according to Eq. (1) the time of its arrival at the cross-section z is

$$\tau = z + t + t_0 = z / \sqrt{1 - (k_1/k)^2} . \tag{19}$$

Recall that the velocity of light in free space in the used system of units is equal to 1. Expressing k through t , we obtain

$$k(t) = \frac{k_1}{\sqrt{1 - \left(\frac{z}{z + t + t_0}\right)^2}} . \tag{20}$$

Figure 6 presents dependences $k(t)$ calculated after Eq. (20) for the cross-section $z = 1000$ with $t_0 = 0, 25$ and 50 . Also shown there is the frequency modulation law (curve 4) calculated for the pulse $u_1(1000, t+1000)$. As can be seen, the $k(t)$ dependence calculated using the rigorous formulas will differ essentially from that calculated after the formula Eq. (20) no matter to what extent the beginning of the wave packets (parameter t_0) is localized in time. Actually, each frequency component of the pulse propagates faster than it is expected proceeding from pure mechanical conception about motion of wave packets. The same conclusion can be derived from the comparison of the $k(t)$ dependence for the pulse $u_1''(t)$ (see Fig. 5(a)) with the frequency modulation law obtained within the kinematical approximation. To that end let us set the input pulse length to $T = 2500$ and its frequency range $k_{\min} \leq k \leq k_{\max}$ to be confined by the following boundaries $k_{\min} = 3.25$ and $k_{\max} = 9$. According to paper

[10], the “fly-in” time t of a wave packet should be related to its group velocity v through the following expression

$$v = v_1 / \left(1 - \left(1 - \frac{v_1}{v_2} \right) \frac{t}{T} \right), \tag{21}$$

where v_1 and v_2 are the group velocities of the wave packets at the frequencies k_{\min} and k_{\max} , respectively. In the case of a regular waveguide the $v(k)$ dependence is given by the formula Eq. (1). Combining Eqs. (1) and (21) we obtain the modulation law of the input pulse which is shown in Fig. 7 by the dashed line. The solid line in the Figure corresponds to the $k(t)$ dependence calculated after the exact formulas. The mere difference in these dependences already makes it impossible to use the kinematical approximation for synthesizing and optimizing real power compressors. Yet more aggravated situation arises in calculating the optimum length L_{opt} of the waveguiding section which would provide, proceeding from the kinematical formulas, the best compression of the input pulse. For the above indicated parameters this length is equal to $L_{opt} = Tv_1v_2 / (v_2 - v_1) \approx 881.14$ [10], which value differs inadmissibly from the exact magnitude $z = 1000$.

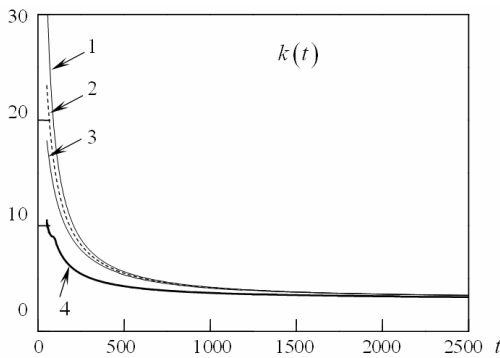


FIG. 6: Dependences $k(t)$ calculated after Eq. (20) for $t_0 = 0$ (curve 1), $t_0 = 25$ (curve 2) and $t_0 = 50$ (curve 3) and the frequency modulation law (curve 4) calculated for the pulse $u_1(1000, t + 1000)$

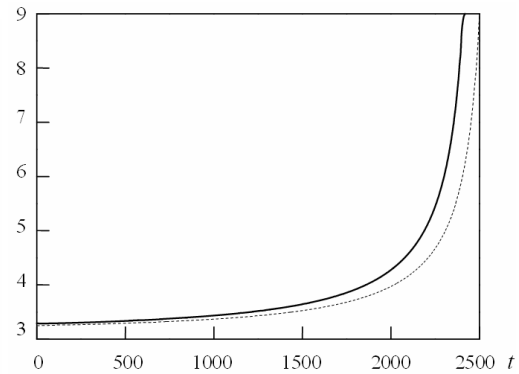


FIG. 7: $k(t)$ dependences calculated for the pulse shown in Fig. 5(a) with the use of the exact formulas (solid line) and the kinematical theory (dashed line)

Thus, the kinematical conception that a radio pulse moves as a superposition of “particles”, proves to be too crude for adequate modeling of physical processes even in such a simple case where the dispersive element is represented by a section of a

regular waveguide. Using this approximation it is impossible to precisely answer the question what should be the frequency and moreover amplitude modulation law of the pulse delivered at the compressor input. This fact plays the role of prime importance for implementing both numerical and full-scale experiments since the knowledge of the dispersion law of a specific device does not imply knowledge of the frequency modulation law of the pulse to be fed at the input of this device.

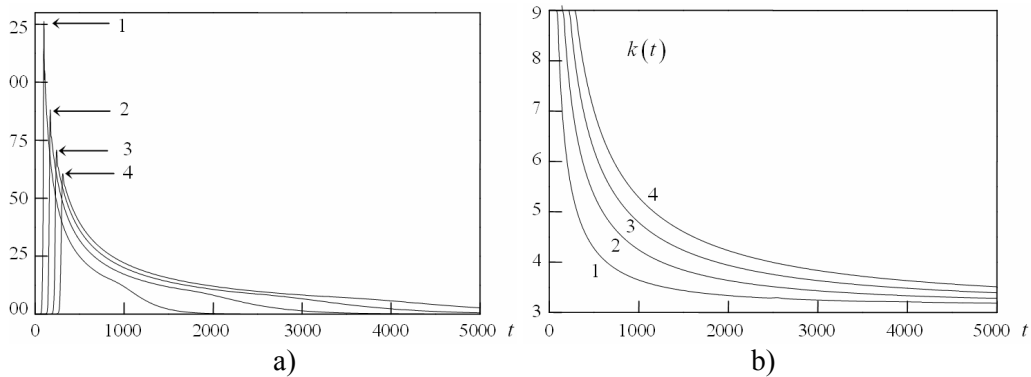


FIG. 8: Amplitude (a) and frequency (b) modulation laws for the pulse $u_1(1000, t + 1000\sqrt{\epsilon})$ calculated for four waveguides filled with a homogeneous nondispersive dielectric material characterized by the permeability $\mu=1$ and conductivity $\sigma=0$. Curves 1, 2, 3 and 4 correspond to $\epsilon=1$ and $a=1$; $\epsilon=4$ and $a=1/2$; $\epsilon=9$ and $a=1/3$; and $\epsilon=16$ and $a=1/4$, respectively

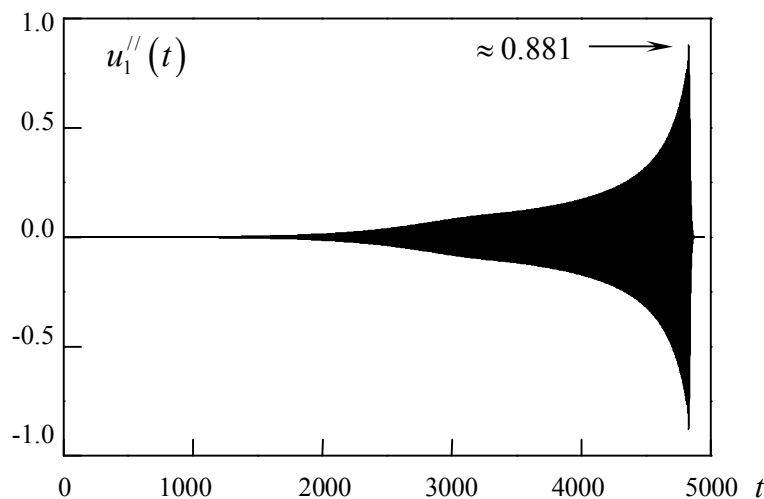


FIG. 9: Time profile of a pulse intended for compression in a parallel-plate waveguide filled by a dielectric material with $\epsilon=4$

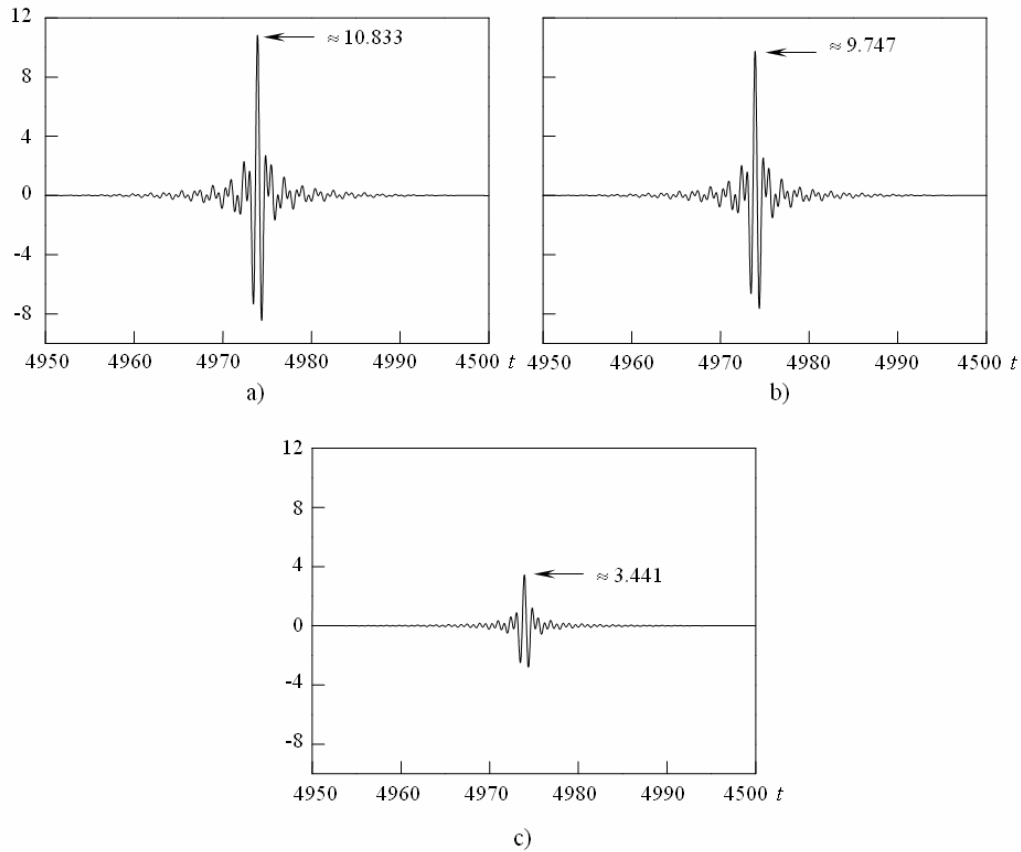


FIG. 10: The pulses $u_1^*(1000, t+1000\sqrt{\varepsilon})$ observed after the pulse shown in Fig. 9 being passed the distance 1000 in waveguides with dielectric filling characterized by $\varepsilon = 4$ and $\sigma = 10^{-7}$ (panel a), $\sigma = 10^{-6}$ (panel b) and $\sigma = 10^{-5}$ (panel c)

Now let us consider the question on the waveguide filling by nondispersive dielectric. The tackling of this question is ambiguous. On the one said this filling makes it possible to attain the greatest frequency separation in initial pulse at that waveguide length when the inverse problem is solved. As was to be expected, the greatest amplitude gain is reached, when the direct problem is solved. On the other hand, the losses in dielectric can reduce to zero this increase in gain. An unambiguous answer on the question on dielectric filling can be received after strong and careful numerical simulation of corresponding electro-dynamical system. Let us illustrate this argument. Figure 8 shows the amplitude and frequency modulation laws which results the propagation at distance $z=1000$ of initial pulse (see Fig. 1(a)) in plane-parallel waveguides, filled with media having $\varepsilon = 1, 4, 9$ and 16. It is supposed that $\mu = 1, \sigma = 0$ and waveguide hate is 1, 1/2 and 1/4 correspondently. With this selection

of the heights the cutoff frequencies and the dispersion law Eq. (1) prove to be identical for all four waveguides. Basically, the cases differ by the optical path lengths passed by the initial pulse. The result is quite expectable. Specifically, the longer the travel path of the pulse, the stronger its spreading in time and space. Now consider the effect of electric loss in the dielectric material filling the waveguide. Let us select the signal obtained for the waveguide with $\varepsilon = 4$ and use it to reconstruct the signal $u_1''(t)$ (Fig. 9) following the above described algorithm to see how its form will be changed after passage the distance $z = 1000$ in the waveguide for different non-zero values of σ . Time profiles of the output pulses calculated for $\sigma = 10^{-7}$, 10^{-6} and 10^{-5} are shown in Fig. 10. This Figure presents maximum magnitudes of the compressed pulses. The respective amplitude gains are equal to $\alpha \approx 12.296$, 11.063 , and 3.906 , while the efficiency factors are $\gamma \approx 0.977$, 0.791 , and 0.102 . It is seen that in the case of sufficiently small σ the use of waveguides with dielectric filling might be more preferable for the pulse compression.

4. CONCLUSIONS

The present paper suggests a rigorous algorithm for calculating transformations of the time profile of electromagnetic pulses propagating in a regular homogeneous waveguide of arbitrary cross-section with perfectly conducting walls. The algorithm has been used for comprehensive analysis of evolution of the signals described by the formulas Eqs. (2) to (5). An efficient computational scheme has been suggested for determining the frequency and amplitude modulation laws of the radio pulses intended for compression in sections of waveguides both hollow and filled with a homogeneous nondispersive dielectric material. It has been shown that the so-called kinematical approximation is inapplicable for rigorous description of propagation of broadband pulse in a dispersive system in the form of superposition of wave packets.

5. APPENDIX: FAST ALGORITHM FOR CALCULATING CONVOLUTION INTEGRALS

To create practicable algorithms of recalculating fields based on the formulas Eqs. (2) to (5) it is necessary to construct an efficient scheme of computing the convolution integrals as follows

$$v(t) = \int_0^t K(t-\tau)u(\tau) d\tau. \quad (\text{A.1})$$

In the general case the function $u(t)$ is specified within the time interval $0 \leq t \leq t_u$, while the function $v(t)$ should be determined within the time interval

$0 \leq t \leq t_v$, with $t_v \geq t_u$. As has been mentioned above, computation of the integral Eq. (A.1) “directly” using the quadrature formulas would require performance of about $O(M^2)$ floating-point operations, where M is the size of the arrays to be convolved. Paper [25] suggested an algorithm for computing such convolution based on the Fast Fourier Transform (FFT) which requires about $O(M \log M)$ operations to be performed. In the Appendix a more computationally efficient modification of this algorithm is described.

Suppose that in the initial time moment we have $u(0) = v(0) = 0$. Let us go over to the mesh functions

$$\begin{aligned} v(t') &\rightarrow v_t, \quad t = 0, 1, 2, \dots, T_v - 1, \quad t' = t \cdot h_t, \quad t_v = (T_v - 1) \cdot h_t, \\ u(t') &\rightarrow u_t, \quad t = 0, 1, 2, \dots, T_u - 1, \quad t' = t \cdot h_t, \quad t_u = (T_u - 1) \cdot h_t, \\ K(t') &\rightarrow K_t, \quad t = 0, 1, 2, \dots, T_v - 1, \quad t' = t \cdot h_t, \end{aligned} \quad (\text{A.2})$$

where h_t is the sampling increment. For simplicity let us set $T_v = T_u$ for the time being and write a discrete analog of Eq. (A.1) using the quadrature trapezoid formula

$$v_0 = 0, \quad v_t = \frac{h_t}{2} \sum_{\tau=0}^t T_\tau \cdot K_{t-\tau} \cdot u_\tau, \quad 0 < t \leq T_u - 1, \quad (\text{A.3})$$

with $T_\tau = 1$, if either $\tau = 0$ or $\tau = t$ and $T_\tau = 2$, if $0 < \tau < t$. Having transformed Eq. (A.3) such that to exclude the factor T_τ under the summation sign, viz.

$$v_0 = 0, \quad v_t = h_t \sum_{\tau=0}^t K_{t-\tau} \cdot u_\tau - \frac{h_t}{2} (K_t \cdot u_0 + K_0 \cdot u_t), \quad 0 < t \leq T_u - 1, \quad (\text{A.4})$$

we will operate in what follows with the sum

$$w_t = \sum_{\tau=0}^t K_{t-\tau} \cdot u_\tau. \quad (\text{A.5})$$

According to [25], let us represent the sum as a product of the lower triangular Toeplitz matrix \mathbf{K} by the column vector of the right-hand part, viz.

$$\mathbf{w} = \mathbf{K} \cdot \mathbf{u}, \quad K_{i,j} = \begin{cases} K_{i-j}, & i \leq j \\ 0, & i < j \end{cases}. \quad (\text{A.6})$$

For example, for $T_u = 14$ the relation Eq. (A.5) can be written as

Then, from applying the convolution theorem to the expression Eq. (A.9) we arrive

$$\mathbf{W} = DFT^{-1} \left[DFT \left[\mathbf{K}^l \right] DFT \left[\mathbf{U} \right] \right], \quad (\text{A.12})$$

where DFT and DFT^{-1} mean respectively, the direct and the inverse discrete Fourier transforms, viz.

$$y_n = DFT \left[\mathbf{X} \right] \equiv \sum_{m=0}^{N-1} x_m e^{-\frac{2\pi i}{N} mn} \quad \leftrightarrow \quad x_m = DFT^{-1} \left[\mathbf{Y} \right] \equiv \frac{1}{N} \sum_{n=0}^{N-1} y_n e^{\frac{2\pi i}{N} mn}. \quad (\text{A.13})$$

If the square matrix size is greater than or equal to a certain s_{FFT} , then computation of the product Eq. (A.8) using the FFT provides gain in speed as compared with the “direct” calculation according to the “row-by-column” rule. The greater is the size of the square matrix in Eq. (A.8) (and, as a result, the greater size of the vectors to be convolved in Eq. (A.9)), the greater advantage can be obtained through performing the matrix multiplication after the formulas Eqs. (A.12) and (A.11). And vice versa, multiplication of small blocks with sizes $s < s_{FFT}$ is more expedient to perform by the “row-by-column” rule since in this case a less number of operations is required than for the FFT-based multiplication. It has been found experimentally that the optimum value is $s_{FFT} = 128$.

The presented algorithm can be additionally optimized. It is easy to ascertain that the multiplication of a square block of arbitrary dimension s representing a lower triangular matrix can be reduced to the circular convolution Eq. (A.9). If s represents a power of two, then it is sufficient to set $K_k = K_{k+1} = \dots = K_{k+s-2} = 0$ in Eqs. (A.8) and (A.10). In the case of an arbitrary s it is more convenient to rewrite Eq. (A.8) in the form of the following product (it has been taken into account here that after partition of the matrix \mathbf{K} into blocks the main diagonals of the all lower triangular matrices will contain the element K_0)

$$\begin{bmatrix} w_i \\ w_{i+1} \\ \dots \\ w_{i+s-1} \end{bmatrix} = \begin{bmatrix} K_0 & & & \\ K_1 & K_0 & & \\ \dots & \dots & \dots & \\ K_{s-1} & \dots & K_1 & K_0 \end{bmatrix} \times \begin{bmatrix} u_j \\ u_{j+1} \\ \dots \\ u_{j+s-1} \end{bmatrix}, \quad (\text{A.14})$$

which can be calculated using the convolution Eq. (A.9) of the two vectors as follows

$$\mathbf{U} = \{u_j, u_{j+1}, \dots, u_{j+s-1}, 0, \dots, 0\} \quad \text{and} \quad \mathbf{K}^l = \{K_0, K_1, \dots, K_{s-1}, 0, \dots, 0\} \quad (\text{A.15})$$

according to the rule

$$w_{i+p} = W_p, \quad p = 0, 1, \dots, s - 1. \tag{A.16}$$

The dimension N of the vectors \mathbf{U} and \mathbf{K}' is equal to the least power of two greater than $2s - 1$.

This is a very important property of the matrix Eq. (A.6) which makes it possible to minimize computational expenses associated with the partition into square blocks and calculation of the FFT plans [28] for each block.

Finally, a more universal rule can be derived. The procedure of partition of the matrix \mathbf{K} in Eq. (A.6) should not necessarily result in square blocks. The multiplication of a rectangular block of size $J \times I$ by a column vector of size J

$$\begin{bmatrix} w_i \\ w_{i+1} \\ \dots \\ w_{i+I-1} \end{bmatrix} = \begin{bmatrix} K_{k+J-1} & \dots & K_{k+1} & K_k \\ K_{k+J} & \dots & K_{k+2} & K_{k+1} \\ \dots & \dots & \dots & \dots \\ K_{k+I+J-2} & \dots & K_{k+I} & K_{k+I-1} \end{bmatrix} \times \begin{bmatrix} u_j \\ u_{j+1} \\ \dots \\ u_{j+J-1} \end{bmatrix} \tag{A.17}$$

(for any rectangular block $k = i - j - J + 1$) can be reduced as well to the circular convolution Eq. (A.9) of the two vectors as follows

$$\mathbf{U} = \{u_j, u_{j+1}, \dots, u_{j+J-1}, 0, \dots, 0\} \text{ and } \mathbf{K}' = \{K_k, K_{k+1}, \dots, K_{k+I+J-1}, 0, \dots, 0\} \tag{A.18}$$

according to the rule

$$w_{i+p} = W_{J-1+p}, \quad p = 0, 1, \dots, I - 1. \tag{A.19}$$

Here the size N of the vectors \mathbf{U} and \mathbf{K}' is equal to the least power of two greater than $I + J - 1$.

Now, let us describe briefly the procedure of partition of the matrix \mathbf{K} into fragments. In the general case with $t_v > t_u$ the function $u(t)$ can be prolonged by zeros to the time moment t_v in order to construct the procedure of partition of the lower triangular matrix as it was done in paper в [25]. However this approach does not seem to be rational. In real physical problems (one of these is considered in the paper) it might be quite possible that t_v is tens and even hundreds times greater than t_u . In this case a greater part of the matrix \mathbf{K} will be multiplied by zero values of the vector \mathbf{U} . However, it is possible to avoid performance of these unnecessary operations. To that end let us complement Eqs. (A.3) and (A.4), respectively, by the expressions

$$v_t = \frac{h_t}{2} \sum_{\tau=0}^{T_u-1} T_\tau \cdot K_{t-\tau} \cdot u_\tau, \quad T_u - 1 < t \leq T_v - 1, \tag{A.20}$$

respect to the longer side. The specific value of N_{max} depends on the capabilities of the specific computer and can be set by the user. In addition, when partitioning rectangular matrices it is necessary to try to obtain blocks in the form as close to the square one as possible since multiplication of square blocks using the FFT provides the maximum computational speedup. To that end rectangular blocks with side ratios greater than 2:1 are as well divided with respect to the longer side such that one of the obtained parts would be a square.

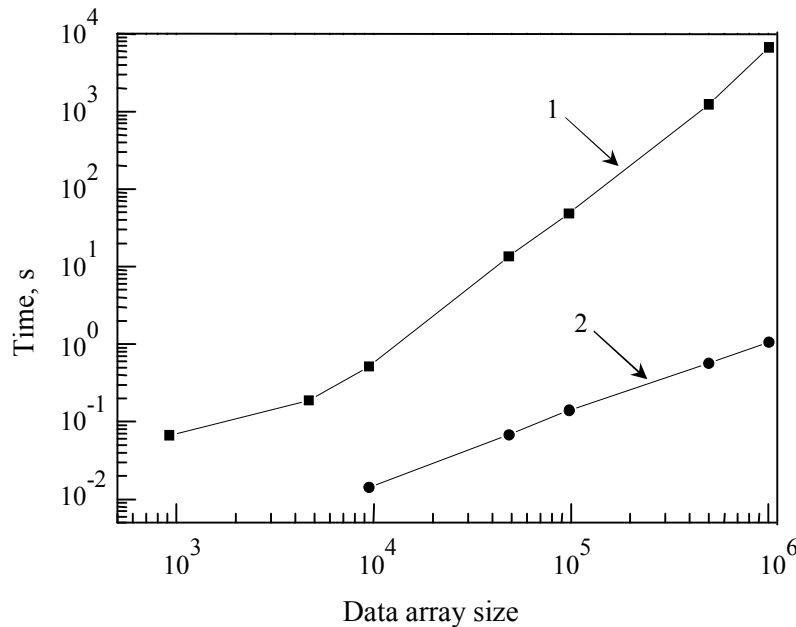


FIG. 11A: Computation time for estimating the convolution integral Eq. (5) for the signal given by Eqs. (13) and (14) in dependence on the input data set size. The calculations have been performed using the quadrature trapezoid formula (curve 1) and the optimized algorithm (curve 2)

After the partition procedure the made lists are browsed and matrix blocks are multiplied by the respective fragments of the vector \mathbf{u} . The multiplication algorithm depends on the size of the respective block. If for a lower triangular matrix lengths of the vectors \mathbf{U} and \mathbf{K}' are less than $2s_{FFT}$, then the block is multiplied by the “row-by-column” rule, otherwise according to the formulas Eqs. (A.12), (A.15) and (A.16). If the number of rows or columns in a complete rectangular block is less than s_{FFT} , then the block is multiplied as well by the “row-by-column” rule, otherwise according to the formulas Eqs. (A.12), (A.18) and (A.19). At that all discrete Fourier transforms are performed using the FFT. The FFT procedures used in this paper have been taken

from website [28]. At last, when the sum Eq. (A.5) has been computed the final values of v_i are determined after the formulas Eqs. (A.4) and (A.21).

The efficiency of the optimized algorithms is illustrated by Fig. 11A. Curve one shows the time of computing the convolution Eq. (5) of the signal Eqs. (13) and (14) directly after the trapezoid formula in dependence on the input array size. Curve 2 corresponds to the time of computing the same convolution using the optimized algorithm. For an array of one million elements in size these times are equal to about 1.78 h and 1 s, respectively. The calculations have been performed using a PC with an Intel Pentium 4 (Prescott) CPU operating at 3 GHz CPU clock.

REFERENCES

1. Ramp, H.O. and Wingrove, E.R., (1961), Principles of pulse compression, *IRE Transaction on military electronics*. **MIL-5(2)**:109-116.
2. Thor, R.C., (1962), A large time-bandwidth product pulse-compression technique, *IRE Transaction on military electronics*. **MIL-6(2)**:169-173.
3. Bongianni, W.L. and Harrington, J.B., (1966), Ultrawide bandwidth pulse compression in YIG, *Proceedings of the IEEE*. **54(8)**:1074-1075.
4. Bromley, R.A. and Callan, B.E., (1967), Use of a waveguide dispersive line in an FM pulse-compression system, *Proceedings of the IEEE*. **114(9)**:1213-1218.
5. Gökgör, H.S. and Minakovic, B., (1971), Circular TE_{01} periodic waveguide as delay line for pulse compression, *Electronics Letters*. **7(20)**:607-608.
6. Shirman, Y.D., (1974), *Signal resolution and compression*, Sov. Radio, Moscow: 360 p. (in Russian).
7. Thirios, E.C., Kaklamani, D.I., and Uzunoglu, N.K., (2004), Pulse compression using a periodically dielectric loaded dispersive waveguide, *Progress in electromagnetic research*. **48**:301-333.
8. Samsonov, S.V., Phelps, A.D.R., Bratman, V.L., Burt, G., Denisov, G.G., Cross, A.W., Ronald, K., He, W., and Yin, H., (2004), Compression of frequency-modulated pulses using helically corrugated waveguides and its potential for generating multigigawatt rf radiation, *Physical review letters*. **92(11)**:118301-1-118301-4.
9. Burt, G., Samsonov, S.V., Bratman, V.L., Denisov, G.G., Phelps, A.D.R., Ronald, K., He, W., Young, A.R., Cross, A.W., and Konoplev, I.V., (2005), Microwave pulse compression using a helically corrugated waveguide, *IEEE Transactions on Plasma Science*. **33(2)**:661-667.
10. Bratman, V.L., Denisov, G.G., Samsonov, S.V., Cross, A.W., Ronald, K., and Phelps, A.D.R., (2007), A technique of obtaining multigigawatt peak power through compression of microwave pulses radiated by a relativistic BWT in a helically corrugated waveguide, *Izvestiya VUZov. Radiofizika*. **50(1)**:40-53 (in Russian).
11. Bratman, V.L., Denisov, G.G., Kolganov, N.G., Mishakin, S.V., Samsonov, S.V., and Sobolev, D.I., (2011), A microwave source of multigigawatt peak power on the basis of a relativistic BWT and a compressor, *Zhurnal tekhnicheskoy fiziki*. **81(2)**:113-117 (in Russian).
12. Mishakin, S.V. and Samsonov, S.V., (2009), Optimized compression of frequency-modulated pulses in a sectioned helically corrugated waveguide, *Zhurnal tekhnicheskoy fiziki*. **79(11)**:93-101 (in Russian).
13. Paseka, O.I., Lobanov, V.E., and Sukhorukov, A.P., (2008), Dynamics of the compression of FM pulses consisting of a small number of field oscillations, *Izvestiya RAS. Seriya fizicheskaya*. **72(12)**:1723-1726 (in Russian).
14. Pazynin, V.L., (2012), On rigorous simulation of frequency-modulated pulses compression in the hollow regular waveguides, *Radiofizika and Elektronika*, **3(3)**:30-34 (in Russian).
15. Nikolsky, V.V., (1961), *Electromagnetic field theory*, Vysshaya shkola, Moscow: 371 p. (in Russian).

16. Maykov, A.R., Sveshnikov, A.G., and Yakunin, S.A., (1986), A finite-difference scheme for nonstationary Maxwell's equations in waveguide systems, *Journal of computational mathematics and mathematical physics*. **26**(6):851-863 (in Russian).
17. Sirenko, Yu.K., Shestopalov, V.P., and Yashina, N.P., (1997), New methods of the dynamic linear theory of open waveguide resonators, *Journal of computational mathematics and mathematical physics*. **37**(7):869-877 (in Russian).
18. Sirenko, Yu.K. and Yashina, N.P., (2003), Time domain theory of open waveguide resonators: canonical problems and generalized matrix technique, *Radio science*. **38**(2):VIC 26-1–VIC 26-12.
19. Sirenko, K.Y. and Sirenko, Y.K., (2005), Exact absorbing conditions in initial boundary-value problems of the theory of open waveguide resonators, *Journal of computational mathematics and mathematical physics*. **45**(3):509-525 (in Russian).
20. Sirenko, K.Y., (2006), Transport operators in axially-symmetric problems of electrodynamics of nonsinusoidal waves, *Elektromagnitnye volny and elektronnye systemy*. **11**(11):15-26 (in Russian).
21. Sirenko, Y.K., (2003), *Modeling and analysis of transient processes in open periodic waveguide and compact resonators*, EDENA, Kharkov: 363 p. (in Russian).
22. Kravchenko, V.F., Sirenko Y.K., and Sirenko, K.Y., (2011), *Electromagnetic wave conversion and radiation by open resonant structures*, FIZMATLIT, Moscow: 320 p. (in Russian).
23. Gradshteyn, I.S. and Ryzhik, I.M., (1980), *Tables of Integrals, Series, and Products*, FL Academic: Orlando. – 1100 p.
24. Abramowitz, M. and Stegun, I.E. (eds.), (1964), *Handbook of mathematical functions with formulas, graphs and mathematical tables*, National Bureau of Standards, Applied Mathematics Series. – 55 p.
25. Sirenko, K., Pazynin, V., Sirenko, Y., and Bageci, H., (2011), An FFT-accelerated FDTD scheme with exact absorbing conditions for characterizing axially symmetric resonant structures, *Progress in Electromagnetic Research*. **111**:331-364.
26. Marple, S.L., (1987), *Digital spectral analysis with applications*, Prentice-Hall, Inc. Englewood Cliffs: New Jersey.
27. Southworth, G.C., (1950), *Principles and application of waveguide transmission*, D.Van Nostrand Co. Inc.: New York.
28. www.fftw.org.